# Supporting Information

## Zaborin et al. 10.1073/pnas.0813199106

### SI Materials and Methods

#### Bacterial Strains

*P. aeruginosa* strains PAO1 and its derivatives were routinely grown in tryptic soy broth (TSB) or *Pseudomonas* Isolation Agar (PIA) supplemented when necessary with tetracycline (Tc), 60 $\mu$g/ml. The PAO1 ΔPqsA/ΔPqsH (ΔPqsAH) double mutant was previously described (1). ΔPhoB was obtained from R. E. W. Hancock (University of British Columbia, Vancouver, BC, Canada); ΔMvfR, ΔPstS, and ΔPhzA1 were obtained from the Washington *P. aeruginosa* transposon mutant library (2), and verified by PCR using the primers recommended by the Mutant Library; ΔPvdD, ΔPchEF, and ΔPvdD/ΔPchEF were obtained from P. Cornelis (Vrije Universiteit Brussel, Brussels) (3). The PAO1 double mutant ΔPhzAG1ΔPhzAG2 was provided by M. Camara (University of Nottingham, UK) and P. Williams (University of Nottingham, UK). The mutant was constructed using the suicide plasmid pDM4 (4) where in frame deletions of both operons were performed (K. Righetti, S.P.D., P. Williams, and M. Camara, unpublished work). In the experiments, the mutants were used with respective wtPAO1 strains.

#### Animals.

**Mouse Model of Gut-Derived Sepsis.** Liver resection in mice was performed as previously described (5) with the following modifications. Six- to 10- week-old male C57BL6 mice weighing between 17.5 and 23 g were obtained from HSD (Harland Sprague–Dawley) Company. All experiments on mice were performed in accordance with University of Chicago guidelines and regulations under protocol number 71744 approved by the Animal Care and Use Committee of the University of Chicago. Mice were fasted 24 h before surgery and then anesthetized using a combination of IP ketamine 100 mg/kg and xylazine 10 mg/kg. Following induction of general anesthesia, a midline laparotomy was performed. The left lobe of the liver was located and placed under gentle traction. A high-temperature cautery pen was then used to remove the left lobe of the liver (approximately 30% of total liver) bloodlessly. The remaining liver was placed back into the abdominal cavity and attention was then focused on locating the ileocecal junction. A 200 $\mu$l suspension of *P. aeruginosa* MPAO1 (approximately $10^8$ CFU/ml) was injected into the lumen of the distal ileum that immediately filled the cecum. Following injection, the intestines were examined for any leakage of contents and then returned to the abdominal cavity. Mice were then closed in 2 layers and allowed to recover. Mice were followed for mortality for 48 h.

**TUNEL Assay and Hemotoxylin and Eosin (H&E) Staining of Intestinal Epithelium in Mice.** Routine 5-$\mu$m paraffin sections of mice ileums were prepared and stained by hemotoxylin and eosin. The TUNEL assay was performed using the Apop Tag Plus Peroxidase in Situ Apoptosis Kit (Millipore Corp.).

**HHQ, HQNO, and PQS Quantification.** HAQs were quantified in the agar of plates with *P. aeruginosa* lawns. The gels were cut into pieces and soaked for 24 h in 10 ml of acetonitrile followed by quantification of HQNO, HHQ, and PQS by HPLC/MS as previously described (6).

**Pyoverdin Assay.** *P. aeruginosa* cells were grown in black, clear bottom 96-well plates (Corning Incorporated, Costar 3603). Pyoverdin was measured by fluorescence at 400 ±10/460 ±40 excitation/emission, using a 96-well Microplate Fluorimeter Plate Reader (Synergy HT, Biotek Inc.), and measurements of relative fluorescence units (RFU) were normalized to cell density measured at 600 nm. Measurements were recorded dynamically up to 24 h. Between measurements, plates were maintained in C24 incubator-shaker (New Brunswick Scientific) set at 37 °C and 100 rpm. Emission spectra at excitation of 400 nm were scanned on Microplate Reader Tecan Safire 2. The specificity of fluorescence for pyoverdin was verified using ΔPvdD mutant deficient in pyoverdin production, in which no fluorescence was found.

**Measurement of Iron in Intestinal Mucus.** Mice were subjected to 30% liver resection without exposure to *P. aeruginosa*. Twenty-four hours later, mice were killed and 10 cm segments of distal ileum were excised and washed with 1 ml of 0.9% NaCl (saline). The intestinal mucus layer was collected by gently scraping the luminal surface of the ileum and suspended in 1 ml of saline. Samples were then homogenized and centrifuged at 5,000 × *g*, 5 min to remove debris. Iron was measured in collected supernatants by standard techniques used in the University of Chicago MedLabs. Briefly, iron was measured using a Roche/Hitachi MOD P automated clinical chemistry analyzer using the FerroZine method. $n = 5$ mice/group, $P = 0.037$

**Real-Time PCR.** To specify the differences in the expression of the 2 highly homologous phenazine biosynthesis operons: PA4210-PA4216 (*phzA1-phzG1*) and PA1899-PA1905 (*phzA2-phzG2*), the Real-Time PCR was performed on the ABI 7900HT System using cDNA (1:20 dilution of cDNA from microarray analysis), SYBR Green qPCR SuperMix-UDG (Invitrogen), and primers: for *pa1900 phzB2*: 5′GGAGTGGTACAACATCAAGGTCTTCGA3′ (unique) and 5′CTCGGGATAGCCGGGGAAGA3′(unique); for *pa4211 phzB1*: 5′GAACATGCCGTCTGGTCATTGAAGT3′ (unique) and 5′CGCATTCGACCCAGAAATGATTG3′(unique); for *pa1899 phzA2*: 5′GAGTACCAACGGTTGAAAGGGTTTACC3′ (unique) and 5′ACCGTTCGGCCCCCTTCA3′ (common between *phzA1* and *phzA2*); for *pa4210 phzA1*: 5′ CAGGGCTATTGCGAGAACCACTACA3′ (common between *phzA1* and *phzA2*) and 5′CACGCAGTTTCTGTATCGGGTTCA3′(unique). Note: *phzA1-G1* and *phzA2-G2* are of 99.3% identity, so we were able to design 2 pairs of unique primers, and 2 pairs of primers where the only one primer was unique. The specificity of primer pairs was verified by melting curves. Expression levels were calculated based on differences in Ct levels.

**QRT-PCR Array.** To determine the expression of multiple genes associated with phosphate and iron signaling, we designed gene specific primers (Tm = 60 °C) to amplify 100 bp fragments of target mRNA. Primers were tested in silica for amplification specificity by BLAST search against the database of *P. aeruginosa* PAO1 genome. Annealing pattern was considered unique if it meets any of 2 criteria: if BLAST search returns a single hit from the database or the region of homology for nonspecific hit has Tm value lower then 50 °C. Selected primer pairs were tested for amplification in vitro. All primers have shown single melting curve and the linear amplification pattern. The primers were used: for *pvdA* (PA2386), PA2386f 5′CCTTCATCGACCTCAACGACAGCTA3′ and PA2386r 5′TCGTTGACGAACGGGCTATCGT 3′; for *fpvA* (PA2398), PA2398f 5′CGCCTACCAGGATAAGCACTCGTT 3′ and PA2398r

5′AAGCATGGTGTCGGGATTCAGATC3′; for *pvdS* (PA2426), PA2426f 5′AAGATGTGGTCCAGGATGCGTTCT3′ and PA2426r 5′TTGCGGACGATCTGGAACAGGTA3′; for *pchF* (PA4225), PA4225f 5′CGACACCCTCTACCGGCTGTTCT3′ and PA4225r 5′GGCGTCCGGCACGAACAG3′; and for *pstS* (PA5369), PA5369f 5′AAGGAAGGCGCTGCCTTCGT3′ and PA5369r 5′TCGGCGCCTTGTTCACGTAGA3′. A gene *tpiA* (PA4748), amplified with primers PA4748f 5′AACAAGCAAGGCGGCATCACA3′ and PA4748r 5′TGCACGGTACGCATTCCAGTGT3′ whose expression did not change in our microarray experiment, was chosen for normalization. RNA was isolated and processed as previously described (7) from *P. aeruginosa* grown for 9 h in NGM ↑ $P_i$ and NGM ↓ $P_i$ adjusted with 0.7 $\mu$M of $Fe^{3+}$ and pH 6.0 as well as the same media complemented with 10 $\mu$M of $Fe^{3+}$. The quality and concentration of RNA was estimated by Nanodrop (NanoDrop Technologies, Inc.) and then 0.5 $\mu$g of total RNA was used in reverse transcription reaction with random primer and SuperScript III (Invitrigen) according to manufacturer recommendations. After 2 h incubation reaction mixtures were diluted 1:20 by nuclease free water and used in qPCR. Each qPCR reaction (10 $\mu$l) was assembled using 0.4 $\mu$M of each primer, 2X SYBR green PCR master mix (Applied Biosystems) and 0.4 $\mu$l of the diluted template. qPCR was performed using 7900HT Fast Real-Time PCR System (Applied Biosystems). The gene expression was normalized to *tpiA* (PA4748) which expression was not influenced by phosphate level as we found in microarray and qPCR array. Finally, fold change was determined using normalized expression in NGM ↑ $P_i$ as 100%.

**The $\beta$-galactosidase Assay.** $\beta$-galactosidase activity in *P. aeruginosa* strains harboring the pGX5 plasmid containing *pqsA'-lacZ* construction and the pGX1 plasmid containing *mvfR'-lacZ* construction was measured as previously described (8). *P. aeruginosa* cells were collected from bacterial lawns growing on NGM ↑ $P_i$ and NGM ↓ $P_i$ agarized media and analyzed for $\beta$-galactosidase activity.

**Lifespan of Nematodes.** *C. elegans* pha-I (e2123), wild type at 15 °C, and embryonic lethal at 25 °C were provided by the *Caenorhabditis* Genetics Center (http://www.cbs.umn.edu/CGC/). Worms were grown at 15 °C on *E. coli* OP50 NGM agarized plates ( ↑ $P_i$ lawns), and adult nematodes were transferred onto experimental plates containing *E. coli* OP50 lawns on NGM ↑ $P_i$ or NGM ↓ $P_i$ agarized media. Worms on experimental plates were incubated at 25 °C, and survival of worms was followed daily. Worms not responding to touch were considered to be dead. Experiments were performed in pentuplicates, data are mean ± SD ($n = 10$), $P > 0.05$ (Student's $t$ test).

**Pyocyanin, PQS, and HHQ Supplementations to *P. aeruginosa* Mutant Lawns.** To examine the effect of pyocyanin supplementation, the pure compound obtained from Cayman Chemical Company was added to ΔPhzAG1ΔPhzAG2 suspension to a final concentration of 100 $\mu$M, and 100 $\mu$l of the suspension was dropped onto NGM ↓ $P_i$ plates. Plates were incubated for 2 days as described above, and prefasted worms were transferred. The development of mortality and redness was examined dynamically. The pyocyanin stock solution (23 mM) was prepared by reconstitution of pyocyanin powder in ethanol as recommended by manufacturer. We chose 100 $\mu$M of pyocyanin based on reports that 10–50 $\mu$M induces oxidative stress in human endothelial cells, and that pyocyanin concentration in sputum ranges between 1 and 130 $\mu$M (9–11).

To examine the effect of PQS and HHQ supplementation, the synthesized pure compounds PQS and HHQ (6) were added to ΔPqsAΔPqsH suspension to a final concentration of 40 $\mu$M followed by the procedure described above.


1. Fletcher MP, et al. (2007) A dual biosensor for 2-alkyl-4-quinolone quorum-sensing signal molecules. *Environ Microbiol* 9:2683–2693.
2. Jacobs MA, et al. (2003) Comprehensive transposon mutant library of Pseudomonas aeruginosa. *Proc Natl Acad Sci USA* 100:14339–14344.
3. Ghysels B, et al. (2004) FpvB, an alternative type I ferripyoverdine receptor of Pseudomonas aeruginosa. *Microbiology* 150:1671–1680.
4. Diggle SP, Winzer K, Lazdunski A, Williams P, Camara M (2002) Advancing the quorum in Pseudomonas aeruginosa: MvaT and the regulation of N-acylhomoserine lactone production and virulence gene expression. *J Bacteriol* 184:2576–2586.
5. Wu L, et al. (2004) High-molecular-weight polyethylene glycol prevents lethal sepsis due to intestinal Pseudomonas aeruginosa. *Gastroenterology* 126:488–498.
6. Lepine F, Deziel E, Milot S, Rahme LG (2003) A stable isotope dilution assay for the quantification of the Pseudomonas quinolone signal in Pseudomonas aeruginosa cultures. *Biochim Biophys Acta* 1622:36–41.
7. Zaborina O, et al. (2008) Structure-Function Aspects of PstS in Multi-Drug-Resistant Pseudomonas aeruginosa. *PLoS Pathog* 4:e43.
8. Zaborina O, et al. (2007) Dynorphin activates quorum sensing quinolone signaling in Pseudomonas aeruginosa. *PLoS Pathog* 3:e35.
9. Muller M (2006) Premature cellular senescence induced by pyocyanin, a redox-active Pseudomonas aeruginosa toxin. *Free Radic Biol Med* 41:1670–1677.
10. Muller M (2002) Pyocyanin induces oxidative stress in human endothelial cells and modulates the glutathione redox cycle. *Free Radic Biol Med* 33:1527–1533.
11. Allen L, et al. (2005) Pyocyanin production by Pseudomonas aeruginosa induces neutrophil apoptosis and impairs neutrophil-mediated host defenses in vivo. *J Immunol* 174:3643–3649.

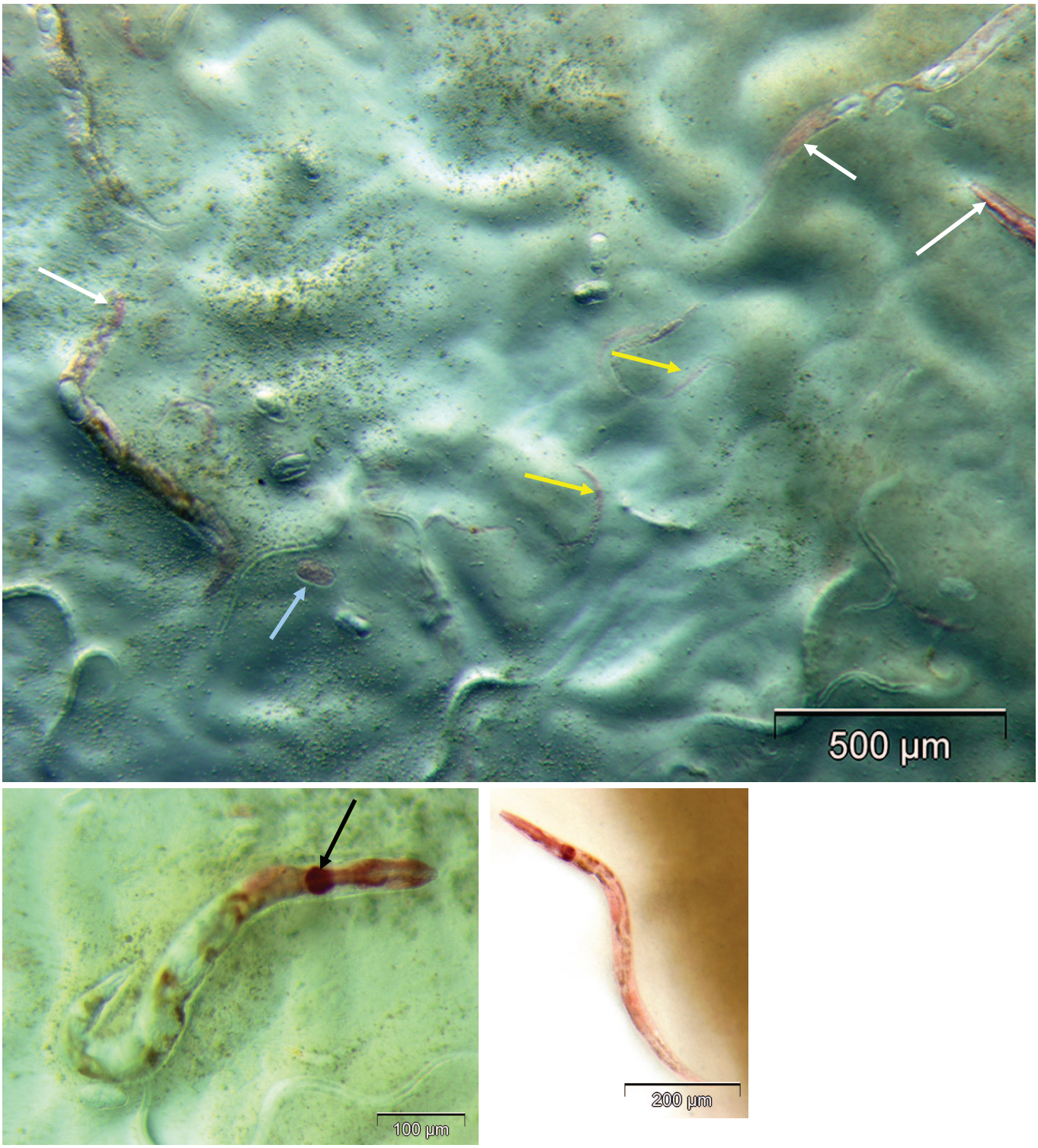


**Fig. S1.** (*Upper*) Red colored material observed within the digestive tube of adult worms (shown by white arrows), larvae (shown by yellow arrows), and in eggs (shown by blue arrow). (*Lower Left*) The most bright red color is seen in pharynx. (*Lower Right*) Red color development in larvae.

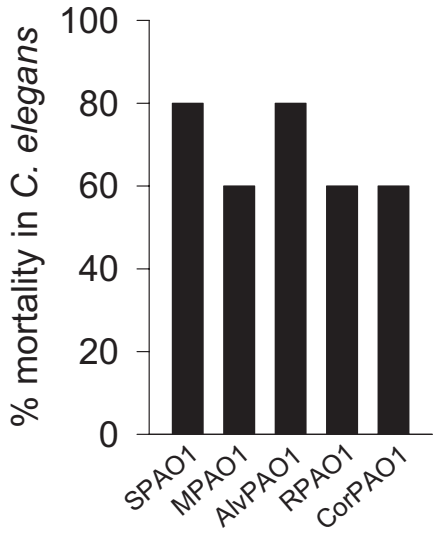


**Fig. S2.** Mortality in *C. elegans* feeding on $\downarrow P_i$ lawns of PAO1 strains obtained from different laboratories. SPAO1 (Steve Diggle, University of Nottingham, Nottingham, UnitedKingdom); MPAO1 (Barbara Iglewski, University of Rochester, Rochester, NY and University of Washington Genome Center, *Pseudomonas aeruginosa* Transposon mutant library, Seattle, WA); AlvPAO1 (John Alverdy, University of Chicago, Chicago, IL); RPAO1 (Cornelia Reimmann, Département de Microbiologie Fondamentale, Biophore, Université de Lausanne, Lausanne, Switzerland), and CorPAO1 (Pierre Cornelis, Vrije Universiteit Brussel, Brussels, Belgium). ($n = 50$ on 3 independent plates/variant).


**Fig. S3.** Redness in the vulva of *C. elegans* (shown by arrow) developed when feeding on *P. aeruginosa* PAO1 low phosphate lawn. Image was created at 60× magnification using the SZX16 Olympus stereomicroscope.

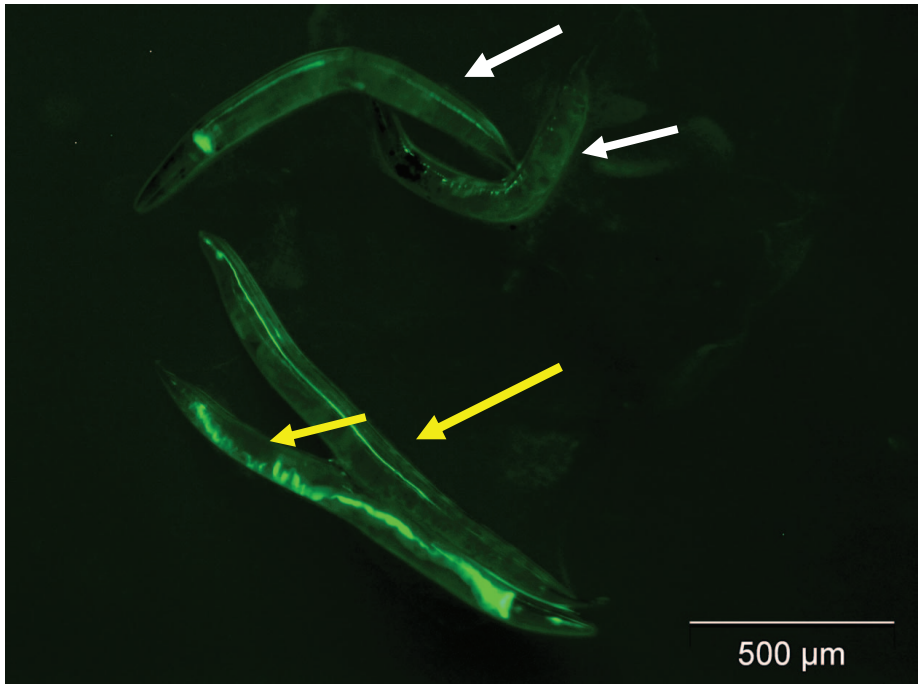


**Fig. S4.** Fluorescent images of nematodes feeding on lawns of *P. aeruginosa* PAO1/EGFP grown on NGM ↓ $P_i$ (shown by white arrow) or NGM ↑ $P_i$ (shown by yellow arrow). Images were created using SZX16 Olympus stereomicroscope.

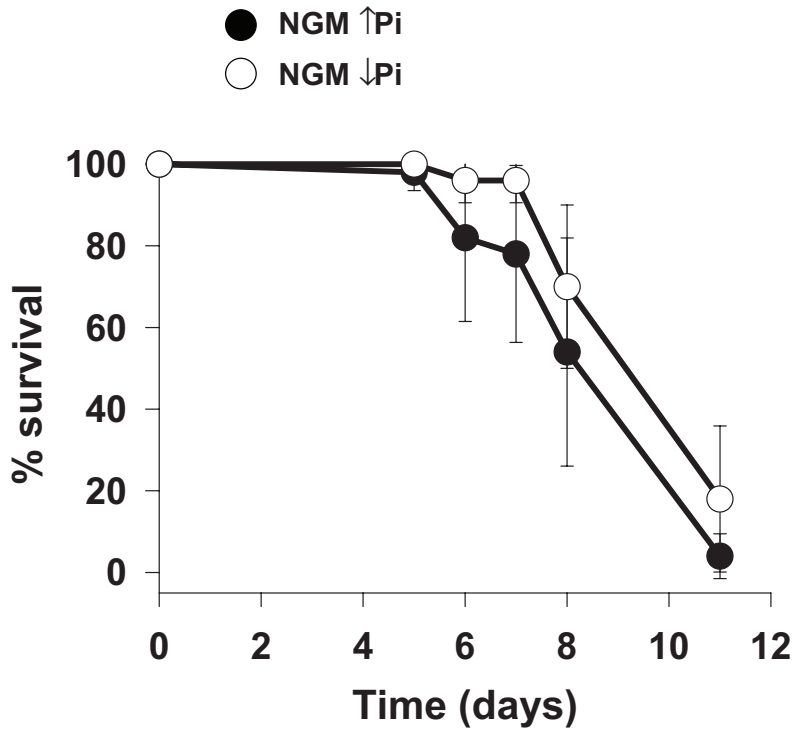


**Fig. S5.** Survival of adult sterile nematodes *C. elegans* pha-1 transferred onto *E. coli* OP50 grown under NGM $\uparrow P_i$ or NGM $\downarrow P_i$ conditions. The mortality of adult pha-1 and N2 was comparable at 25 °C.

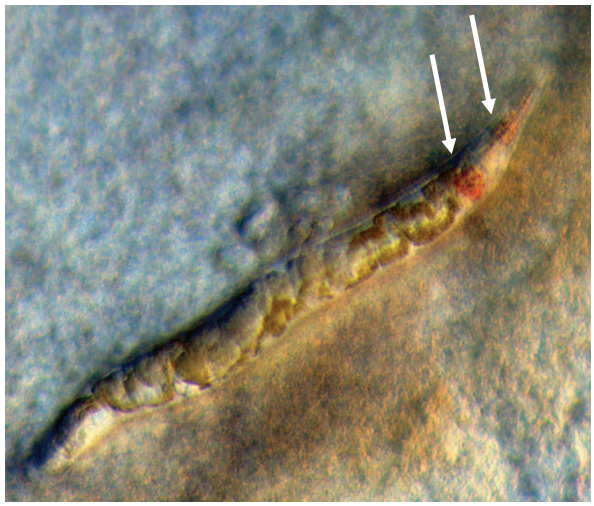

**Fig. S6.** PQS supplementation restores mortality in *C. elegans* feeding on ΔPqsAΔPqsH (ΔPqsAH) NGM ↓ $P_i$ lawns that was correlated with the appearance of red spots within the pharynx of *C. elegans* (shown by white arrows).

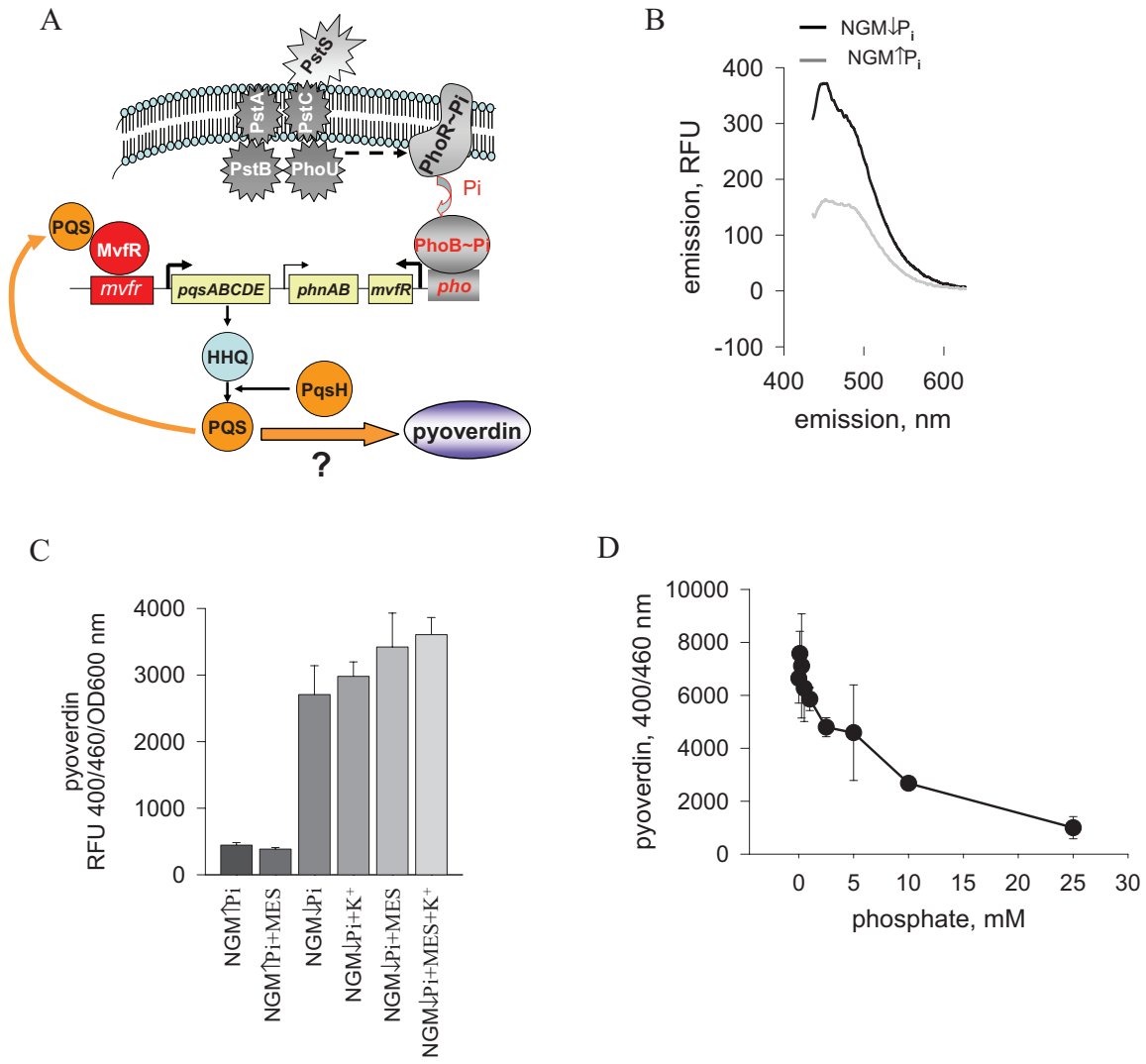


**Fig. S7.** (*A*) Schemata of hypothesized pathway linking phosphate signaling and pyoverdin production. *P. aeruginosa* senses a low extracellular phosphate via PstS protein. The production of PstS is induced under low phosphate conditions leading to conformational changes in Pst proteins [based on the dynamic model of phosphate starvation response proposed by Van Dien and Keasling (*J Theor Biol* 190:37–49)]. These conformational changes are sensed by the product of the fifth gene of the *pst* operon, PhoU, that leads to the release and autophosphorylation of a 2-component sensor histidine kinase PhoR and sequential phosphorylation of a 2-component response regulator PhoB. The phosphorylated transcriptional regulator PhoB~P then binds to a specific *pho* box and changes the expression of multiple genes. Activation of *mvfR* under low phosphate conditions is likely mediated by PhoB regulation via *pho* box located upstream of *mvfR*. MvfR in turn activates the expression of *pqs* operon leading to the production of HHQ, a precursor of PQS. PQS binding to MvfR further accelerates *pqs* expression leading to increased PQS production. PQS chelates iron leading to iron limitation and therefore pyoverdin production. (*B*) Emission spectra at 400 nm excitation of *P. aeruginosa* PAO1 after 3 h of growth in NGM ↓ $P_i$ and NGM ↑ $P_i$ liquid media. (*C*) Effect of replenishments of NGM ↓ $P_i$ liquid media with 25 mM KCl and/or 25 mM Mes, pH 6.0 on pyoverdin production. (*D*) Dose dependent effect of phosphate on pyoverdin production at varying concentrations of K-Ph buffer added to NGM ↓ $P_i$ while keeping constant pH of 6.0 with 25 mM Mes buffer.

## Other Supporting Information Files

Table S1
Table S2
Table S3
Table S4